

Supporting Information

**Macroscopically Aligned Graphite Films Prepared from
Iodine-Doped Stretchable Polyacetylene Films Using
Morphology-Retaining Carbonization**

Satoshi Matsushita and Kazuo Akagi*

Department of Polymer Chemistry, Kyoto University, Katsura, Kyoto 615-8510, Japan

1. Materials and Measurements

1.1. Materials

1.2. Measurements

2. Polymerization of Acetylene

2.1. S-Type PA Film

2.2. Stretchable PA Film

3. Electrical conductivity and stability as a function of stretching degree

Supporting References

Supporting Figures

1. Materials and Measurements

1.1. Materials. The chemical compounds were purchased from commercially available sources and were used as received. Hydrochloric acid (HCl), iodine (I₂), fuming nitric acid (HNO₃), and sodium (Na) were purchased from Nacalai Tesque, Inc. Calcium hydride (CaH₂) was purchased from Wako Pure Chemical Industries, Ltd. The titanium compound, *tetra-n*-butoxytitanium [Ti(O-*n*-Bu)₄], was purchased from Sigma-Aldrich Co., Ltd, and it distilled under reduced pressure prior to use. The alkylaluminum compound, triethylaluminum (AlEt₃), was purchased from Nippon Aluminum Alkyls, Ltd. Aluminum powder was purchased from Nilaco Co., Ltd. Toluene and cumene were distilled over sodium as a drying agent under argon gas prior to use. Ethanol (EtOH) and methanol (MeOH) (Nacalai Tesque, Inc.) were used as received. Tetrahydrofuran (THF) was distilled over calcium hydride as a drying agent under argon gas prior to use. Acetylene gas of six-nine grade was purchased from Koatsu Gas Kogyo Co., Ltd. All experiments were performed under an argon (>99.99% purity) atmosphere. Polyimide tape [P-221, thickness (*t*): 69 μm] was purchased from Nitto Denko, Co. Glass capillary tubes were purchased from Hilgenberg GmbH (Hilgenberg Mark-tubes; length 80 mm, O.D. 1.00 mm, wall 0.01 mm).

1.2. Measurements. Elemental analysis (EA) was performed at the Center for Organic Elemental Microanalysis of Kyoto University.

The thermal behaviors of polyacetylene (PA) and graphite films were investigated in heating runs

performed at a heating rate of 10 °C/min under flowing nitrogen gas using a thermogravimetric-differential thermal analysis (TG-DTA) apparatus (TG-DTA6200, Seiko) with platinum pans.

X-ray diffraction (XRD) measurements were performed using a Rigaku ultra-X18 diffractometer. XRD patterns were recorded using an X-ray generator with Ni-filtered CuK α radiation (40 kV/300 mA: $\lambda = 1.54 \text{ \AA}$) and a flat-plate camera (RINT2500, Rigaku). The sample-to-film distance was 100 mm as calibrated using the (111) face of aluminum ($d = 2.33787 \text{ \AA}$), and the exposure time was 60–240 min. The diffraction pattern was recorded on an imaging plate and scanned by an R-Axis DS3A or an RAXIA-Di imaging plate reader at 100 μm resolution. The crystal size along the c -axis (L_c) of the graphite film was estimated from the (002) diffraction peak in the XRD pattern using the Scherrer equation: $L = K\lambda/\beta\cos\theta$, where K is the shape factor and adopted to be 0.94, λ is the X-ray wavelength, β is the peak width at half maximum in radians, and θ is the Bragg angle.¹ The azimuthal-angle profiles were generated using Rigaku 2DP[®] software (Ver.2.0.1). The peak width at half maximum was calculated using the software Origin[®] 8.5.

Raman spectra were obtained at room temperature using the backscattering method via a spectroscopy with a triple monochromator and a charge-coupled device (CCD) detector cooled by a Peltier device (NRS-2100, JASCO). A 100 mW argon ion laser with a wavelength of 514.5 nm was used. The exposure time was 30–120 sec (10–30 sec \times 3–4). The NRS-4100 Raman spectrometer was also used [1.6 mW, 532 nm, 60 sec (30 sec \times 2)]. The crystal sizes along the a -axis (L_a) of the

carbon and graphite films were estimated from the Raman spectra using the following equation: $L_a = 4.35(I_D/I_G)^{-1}$, where I_D and I_G are the integrated intensities of the D-band and G-band, respectively.^{2,3} The Raman spectra were fitted with a mixed Gaussian-Lorentzian function using the software PeakFit®.

The film thickness was measured using a Nikon Digimicro digital length measuring system with DIGIMICRO MH-15M, DIGIMICRO STAND MS-5C, and DIGITAL READOUT UC-101.

The tensile and three-point bending tests of the carbon films were performed at room temperature using a TENSILON RTG-1210 (A&D) with a load cell of 500 N at a displacement rate of 0.05 mm/min for the tensile test and 2 mm/min for the bending test. The specimens for the tensile test were 4–12 mm wide (w), and the chuck distance (L_t) was 5 mm. The specimens for the bending test were 9–14 mm wide (w), and the distance between supporting points (L_b) was 22 mm. Five measurements were conducted for each sample. The tensile strength (σ_t) and modulus (ε_t) were calculated using, $\sigma_t = f_t/wt$ and $\varepsilon_t = f/\delta$, respectively, where f_t is the maximum load, t is the specimen thickness, and f/δ is the initial linear slope of the load displacement curve. The bending strength (σ_b) and modulus (ε_b) were calculated using, $\sigma_b = 3f_b L_b / 2wt^2$ and $\varepsilon_b = L_b^3 f / 4wt^3 \delta$, respectively.

The electrical conductivities of the PA and carbon films were measured at room temperature using a low resistivity meter, Loresta GP with a MCP-TP06P probe (Mitsubishi Chemical Analytech).

Infrared (IR) absorption spectra of the PA and graphite films were measured in film form or in powdery solid state using a JASCO FT (Fourier transform)-IR 4200 spectrometer with an E082PL-82 polarized cell using transmission or ATR mode. When the sample was measured in the powdery solid

state, the measurement was performed using the KBr method. The *cis* content of the PA film was evaluated using the following equation: *cis* content (%) = $100[1.30A_{cis}/(1.30A_{cis}+A_{trans})]$, where A_{cis} and A_{trans} represent the absorbances of the 740 and 1015 cm^{-1} bands in the spectrum of a specimen, respectively.⁴

The accelerating voltage of the field emission (FE)-SEM (JSM-7500F, JEOL) was 2–10 kV. The PA and carbon films were coated with Pt or Pt-Pd alloy using a JFC-1600 (JEOL) ion coater prior to SEM measurements. The coating thickness was determined to be ca. 5 nm.

The carbonization and graphitization were performed using an electric furnace (KDF75, Denken) and a graphitizing apparatus (Sanriko denki) or SCC-U-80/150 (2P) (Kurata Giken), respectively.

The carbonization and graphitization yields were determined using the equations: $100[(\text{weight of carbonized PA film})/(\text{weight of PA film})]$ and $100[(\text{weight of graphitized film})/(\text{weight of carbon film})]$, respectively. The total yield of a graphite film was calculated on the basis of carbonization (800 °C) and graphitization (1400–3000 °C) yields. The carbonization yield is only in the case of fully doped PA films used as carbonization precursors.

The mechanical stretching procedure was performed in a glove box (MDB-1B, MIWA MFG Co., Ltd.) filled with nitrogen gas at room temperature.

2. Polymerization of Acetylene

2.1. S-Type PA Film. All experiments were performed under an atmosphere of argon gas of six-nine

grade. Typical Shirakawa-type (S-type) PA films were generally synthesized as follows. Toluene was used as a solvent for the Ziegler–Natta catalyst, *tetra-n*-butoxytitanium, $\text{Ti}(\text{O-}n\text{-Bu})_4$, and triethylaluminum, AlEt_3 . The total amount of solvent was 2 ml. The typical concentration of $[\text{Ti}]$ was ~ 0.4 mol/l, and the mole ratio of the cocatalyst-to-catalyst $[\text{Al}]/[\text{Ti}]$ was approximately 4. The catalyst solution was aged for 40 min in a Schlenk flask at ambient temperature. The catalyst solution was coated onto the inner wall of the Schlenk flask by slowly rotating the flask after aging. The flask was connected to a vacuum line via a flexible joint and then degassed. The interfacial polymerization was performed by introducing acetylene gas into the catalyst solution. Acetylene gas of six-nine grade was used without further purification. The polymerization temperature was maintained constant at -78 °C by immersing the Schlenk flask into a dry ice–ethanol bath. The initial acetylene pressure was 561 Torr. The polymerization was stopped when the pressure decreased by 74 Torr. The polymerization time was 60 min. The resulting PA film was carefully stripped from the container and washed with purified toluene, a methanol (MeOH) solution containing 1 N HCl, and THF sequentially at -78 °C. The film was dried by vacuum pumping on a Teflon (polytetrafluoroethylene) sheet for >2 h and was stored in a freezer at -20 °C. The thickness of the film was 84 ± 4 μm . EA indicated that the PA film had carbon and hydrogen contents of 88.54 and 7.48 wt. %, respectively (Calcd. C 92.26, H 7.74.). The bulk density of the PA film was 0.71 g/cm^3 (d_{true} : 1.16 g/cm^3).⁵ The present PA film had a *cis* content of 87% (Figure S1a). The electrical conductivity of the PA film was 330 ± 140 S/cm (t : 89 ± 9 μm , probe: MCP-TPQPP) after iodine doping ($[\text{CHI}_{0.20}]_n$) at room temperature.

2.2. Stretchable PA Film. The stretchable PA films were generally synthesized as follows. The solvent containing the catalyst ($[Ti] = \sim 1$ mol/l, $[Al]/[Ti] = \sim 2$, and aging time = 65 min) was prepared in a Schlenk flask. Cumene was used as a solvent for the catalyst. The catalyst solution was further aged for 180 min at a high temperature of 150 °C following the room-temperature aging. The acetylene polymerization was conducted at -78 °C on the reaction field by introducing the acetylene gas into the flask for 24 h. The initial pressure of the acetylene gas was 559 Torr. Finally, a film thickness of 26 ± 4 μm was obtained. EA indicated that the PA film had carbon and hydrogen contents of 89.02 and 7.58 wt. %, respectively (Calcd. C 92.26, H 7.74.). The bulk density of the PA film was 1.16 g/cm³. The present PA film had a *cis* content of 87% (Figure S1b). The electrical conductivity of the unstretched PA film was 499 ± 103 S/cm (t : 56 ± 5 μm) following iodine doping ($[\text{CHI}_{0.25}]_n$) at room temperature.

3. Electrical conductivity and stability as a function of stretching degree

Table S2 presents electrical conductivity of the carbon and graphite films as a function of stretching degree. Photographs of the stretchable PA films with various stretching degree before and after the carbonization at 800 °C were also presented in Figure S17. According to the literature, the electrical conductivity of the iodine-doped stretchable PA film increases with increasing degree of stretching.⁶ This is because a uniaxial alignment of the polymer chain occurs along the stretching direction

associated with the mechanical stretching of the film. In contrast, the stretchable PA film carbonized at 800 °C shows a conductivity of 21–44 S/cm irrespective of the stretching degree. This is due to the intrinsic amorphous nature of the carbon film. The subsequent graphitization of the carbon film provides the graphite film with an improved conductivity. The graphite film prepared from the stretched (l/l_0 : ca. 4) PA film at 2600 °C shows a conductivity of 539 S/cm along the stretching direction and the unstretched PA film graphitized at 2600 °C shows that of 282 S/cm. It is clear that the former shows approximately 1.9 times higher conductivity than the latter. Figures S18 and S19 show the TG analysis of the carbon and graphite films, respectively, showing the stability of the films.

Supporting References

- (1) Biscoe, J.; Warren, B. E. *J. Appl. Phys.* **1942**, *13*, 364–371.
- (2) Tuinstra, F.; Koenig, J. L. *J. Chem. Phys.* **1970**, *53*, 1126–1130.
- (3) Knight, D. S.; White, W. B. *J. Mater. Res.* **1989**, *4*, 385–393.
- (4) Ito, T.; Shirakawa, H.; Ikeda, S. *J. Polym. Sci., Polym. Chem. Ed.* **1974**, *12*, 11–20.
- (5) Abadie, M. J. M.; Hacene, S. M. B.; Cadene, M.; Rolland, M. *Polymer* **1986**, *27*, 2003–2008.
- (6) Akagi, K.; Suezaki, M.; Shirakawa, H.; Kyotani, H.; Shimomura, M.; Tanabe, Y. *Synth. Met.* **1989**, *28*, D1–D10.

Supporting Figures

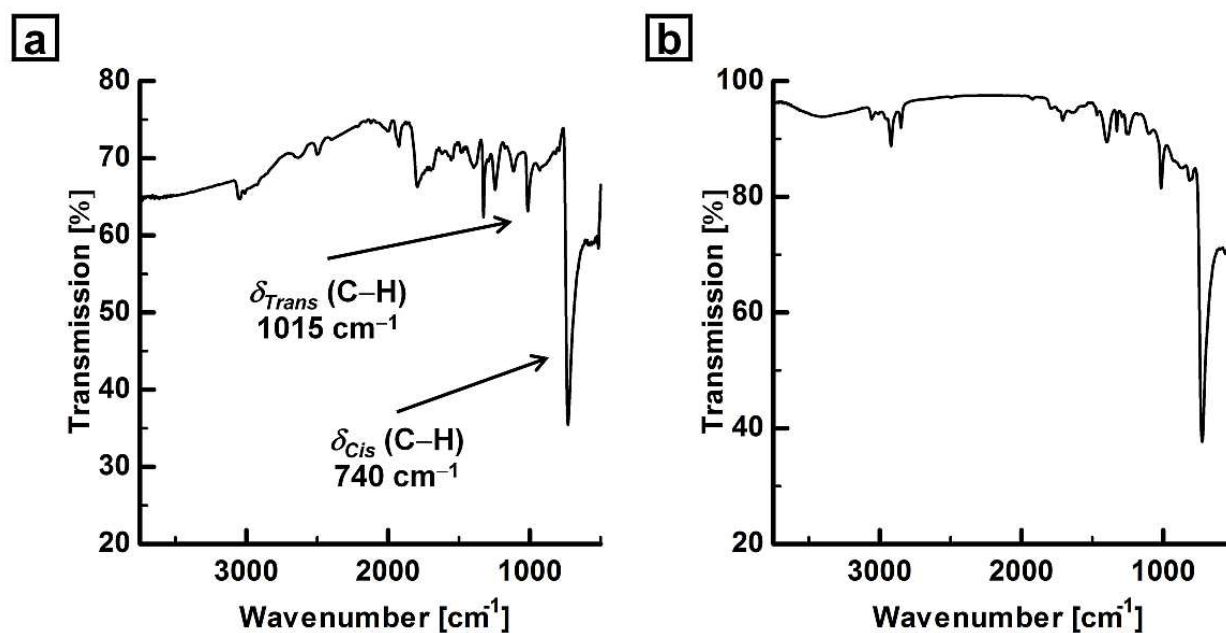


Figure S1. (a) ATR-IR absorption spectrum of the typical PA film. The *cis* content of 87% was calculated from the absorption bands at 740 and 1015 cm^{-1} attributed to *cis* and *trans* C–H out-of-plane vibrations, respectively. (b) ATR-IR absorption spectrum of the stretchable PA film. The *cis* content was calculated to be 87%.

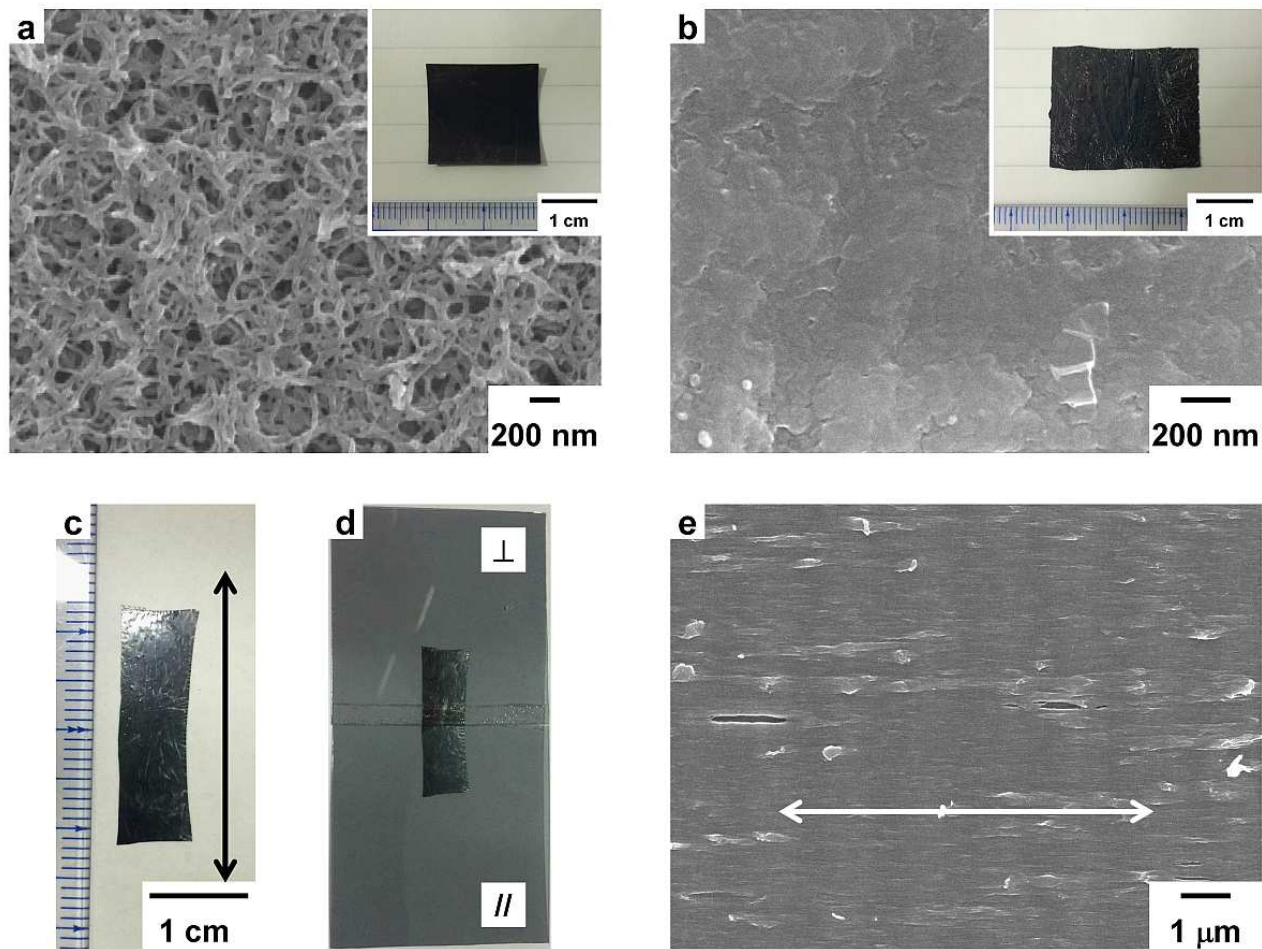


Figure S2. SEM images of the (a) S-type (gas side), (b) unstretched, and (e) mechanically stretched PA films ($[\text{CHI}_{0.26-0.33}]_n$) carbonized at 800 °C. The insets show photographs of the (a) S-type [precursor: $[\text{CHI}_{0.30}]_n$, gas side, t : $62 \pm 2 \mu\text{m}$, bulk density (d_{bulk}): 1.20 g/cm^3 , electrical conductivity (σ): $42 \pm 1 \text{ S/cm}$] and (b) unstretched ($[\text{CHI}_{0.26}]_n$, t : $45 \pm 9 \mu\text{m}$, d_{bulk} : 1.08 g/cm^3 , σ : $58 \pm 5 \text{ S/cm}$) PA films carbonized at 800 °C. Photographs of the (c) stretched PA film ($[\text{CHI}_{0.34}]_n$, t : $18 \pm 0 \mu\text{m}$, d_{bulk} : 1.24 g/cm^3 , $\sigma_{//}$: $66 \pm 2 \text{ S/cm}$) carbonized at 800 °C and the (d) aligned carbon film with polarizers.

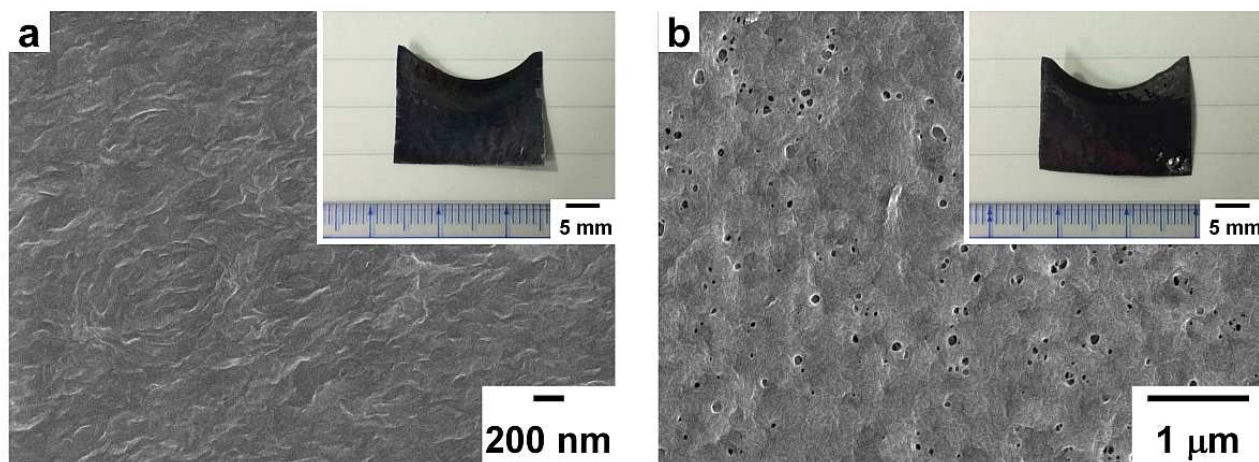


Figure S3. SEM images of the (a) gas and (b) glass sides of typical PA film graphitized at 2600 °C. The insets show photographs of (a) gas and (b) glass sides of the graphite film ($[\text{CHI}_{0.08}]_n$, t : 35 ± 4 μm , σ : 494 ± 26 S/cm).

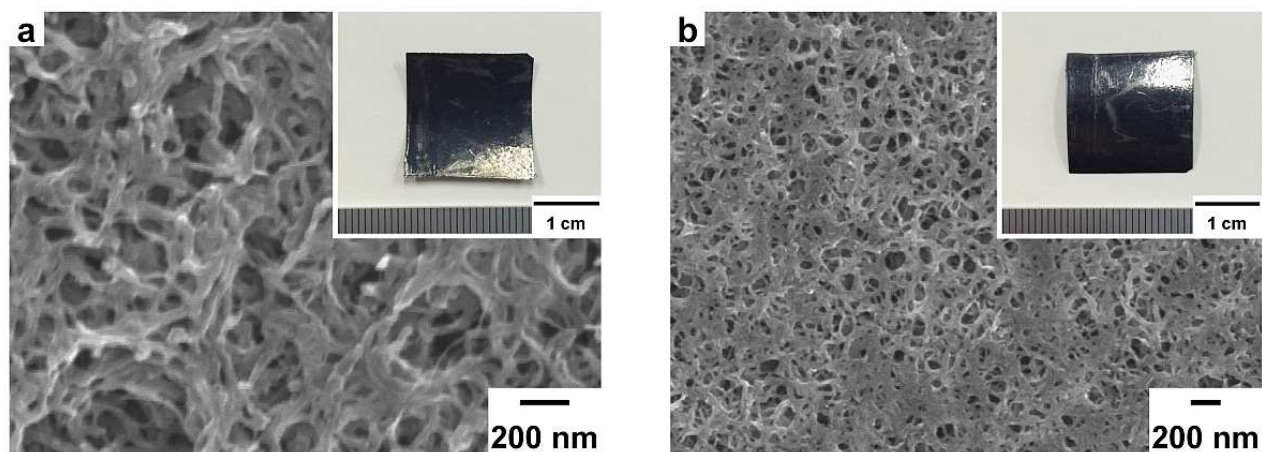


Figure S4. SEM images of the (a) gas and (b) glass sides of the typical PA film graphitized at 3000 °C, respectively. The insets show photographs of the graphite film ($[\text{CHI}_{0.26}]_n$, t : 74 ± 1 μm , d_{bulk} : 1.12 g/cm³, σ : 225 ± 9 S/cm) with (a) gas-side and (b) glass-side surface morphologies, respectively.

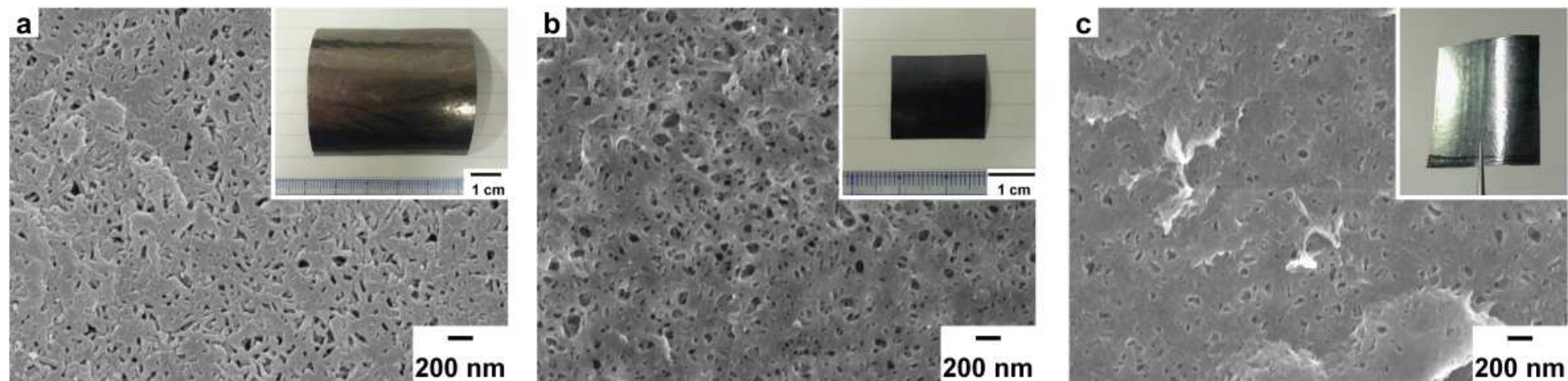


Figure S5. SEM images of glass side of the (a) untreated typical PA, (b) carbon ($[\text{CHI}_{0.30}]_n$, 800 °C), and (c) graphite ($[\text{CHI}_{0.27}]_n$, 2600 °C) films. The insets show photographs of glass side of the (a) untreated typical PA (t : 101 ± 5 μm , d_{bulk} : 0.67 g/cm^3), (b) carbon ($[\text{CHI}_{0.30}]_n$, 800 °C, t : 62 ± 2 μm , d_{bulk} : 1.20 g/cm^3 , σ : 42 ± 1 S/cm), and (c) graphite ($[\text{CHI}_{0.27}]_n$, 2600 °C, t : 55 ± 6 μm , d_{bulk} : 1.32 g/cm^3 , σ : 257 ± 22 S/cm) films.

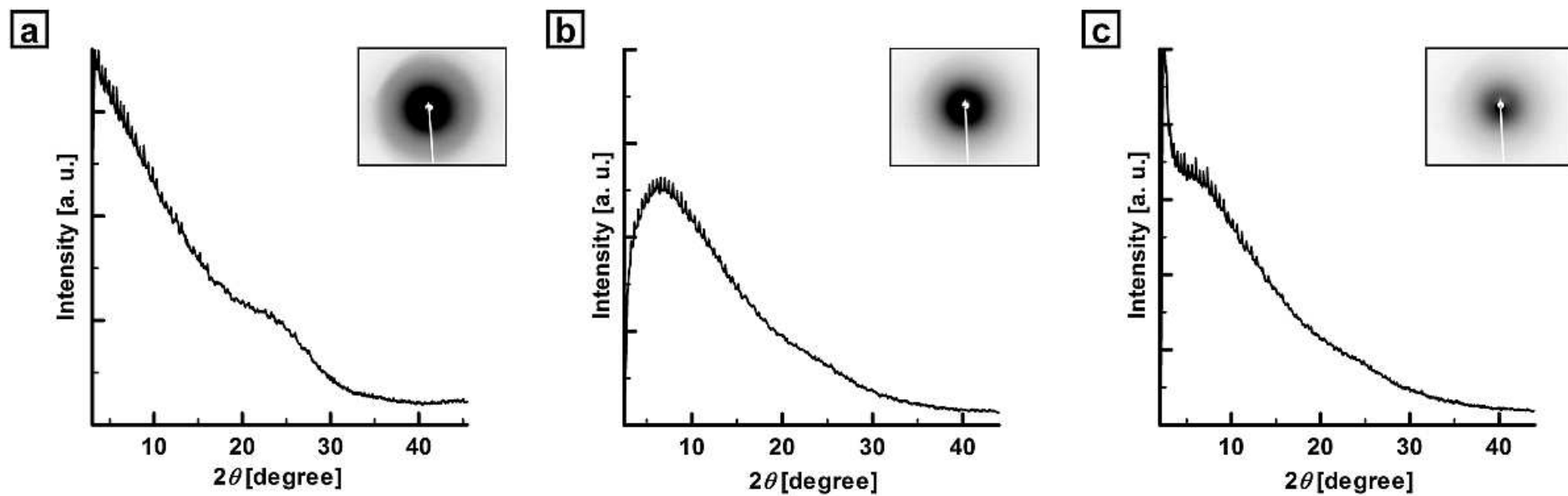


Figure S6. XRD patterns of the (a) S-type, (b) unstretched, and (c) mechanically stretched PA films ($[\text{CHI}_{0.26-0.35}]_n$) carbonized at 800 °C. The incident X-rays are perpendicular to the film surface.

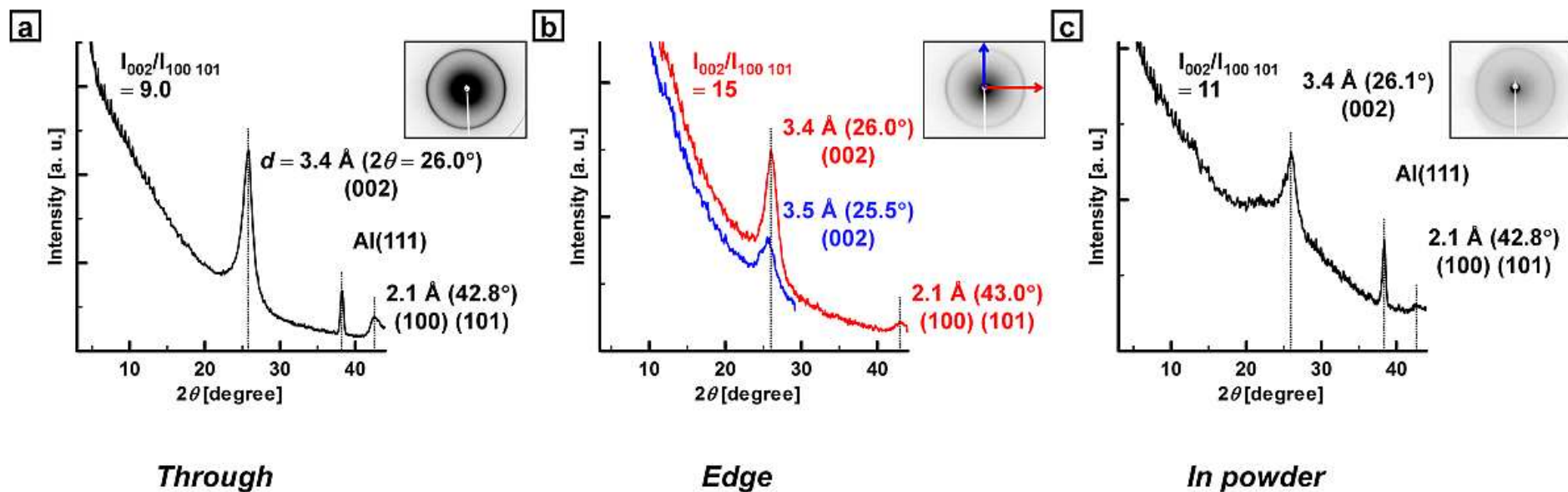


Figure S7. XRD patterns of the typical PA films ($[\text{CHI}_{0.24-0.27}]_n$) graphitized at 2600 °C in (a) through and (b) edge directions and measured in (c) powder form.

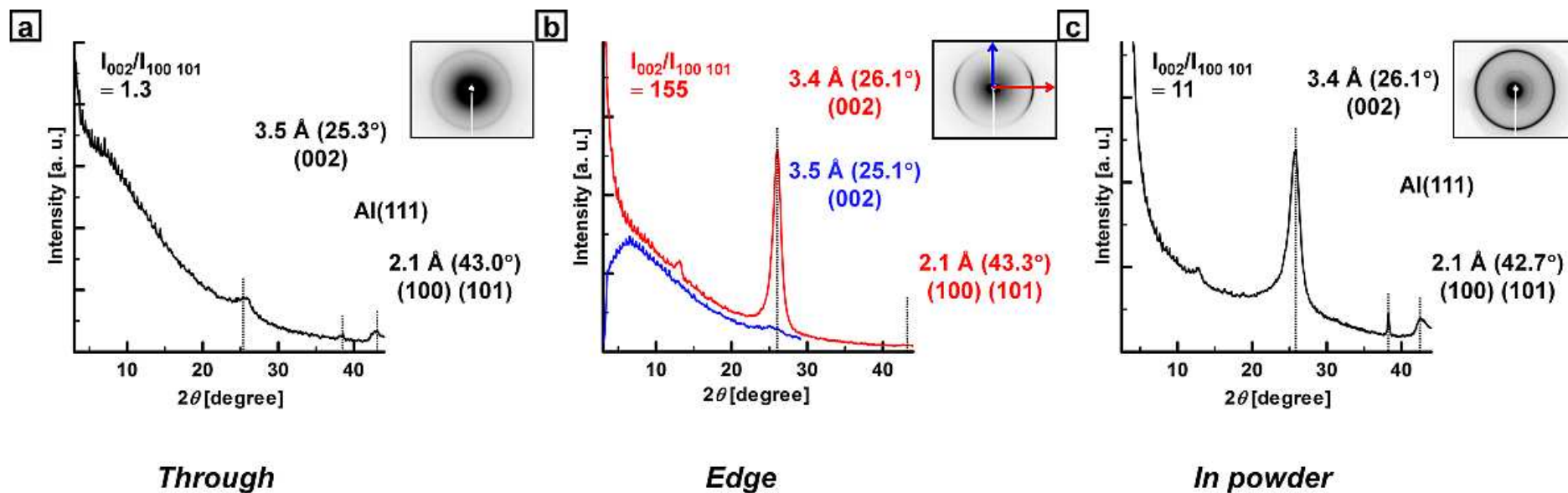


Figure S8. XRD patterns of the unstretched PA film ($[\text{CHI}_{0.26}]_n$) graphitized at 2600 °C in (a) through and (b) edge directions and measured in (c) powder form.

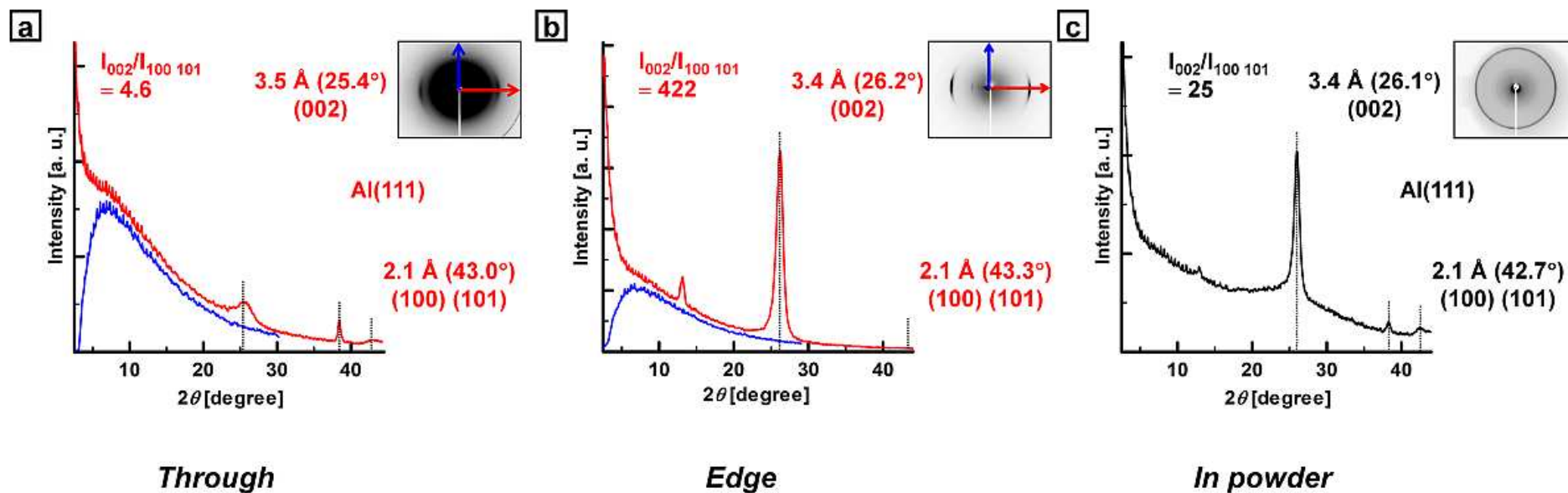


Figure S9. XRD patterns of the mechanically stretched PA film ($[\text{CHI}_{0.33-0.36}]_n$) graphitized at 2600 °C in (a) through and (b) edge directions and measured in (c) powder form.

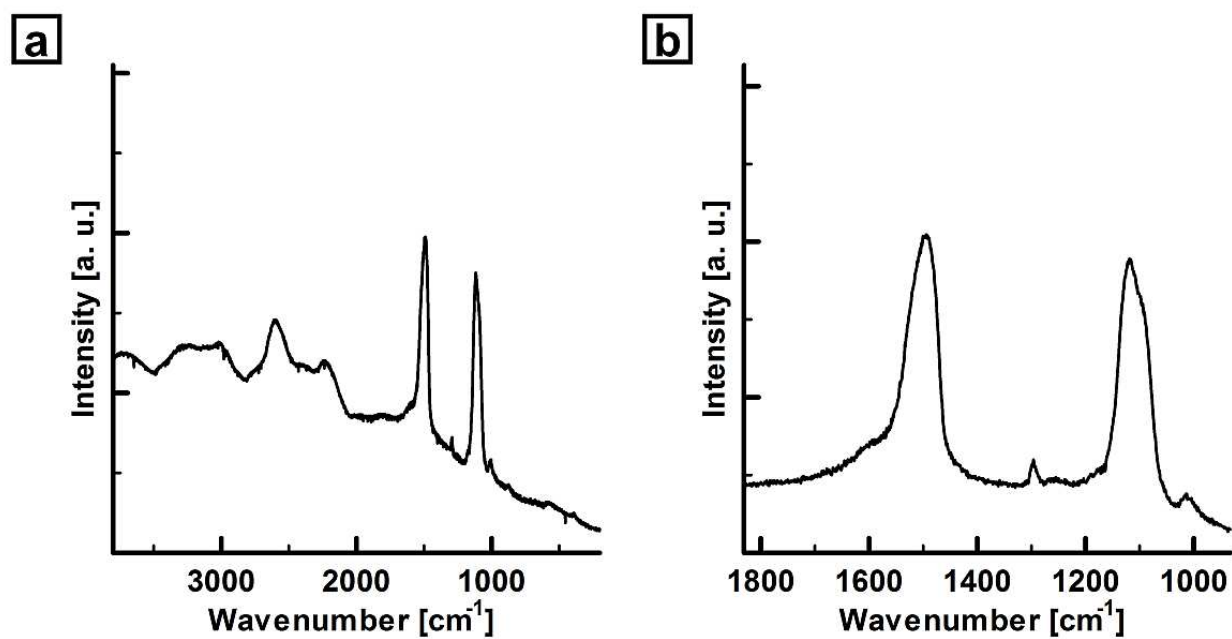


Figure S10. (a) Raman scattering spectrum of the typical PA film and (b) its magnified spectrum.

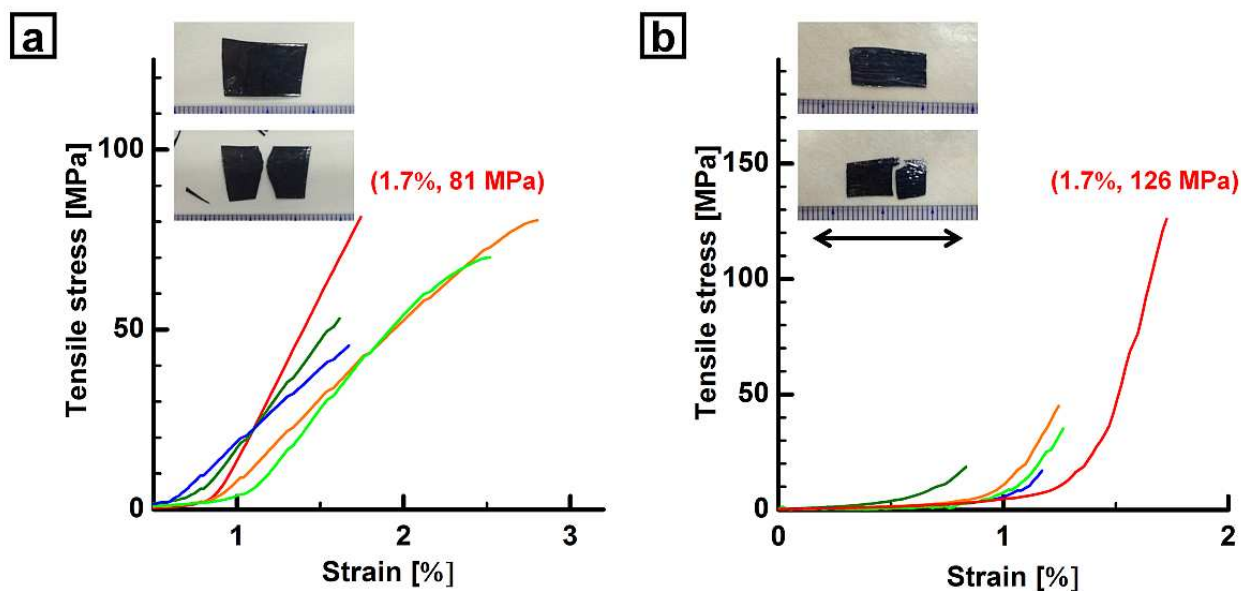


Figure S11. (a) The stress–strain curves for five different tensile test measurements of the carbon film (t : 29–97 μm) prepared from the typical PA film $[(\text{CHI}_{0.23-0.28})_n]$ at 800 $^{\circ}\text{C}$. (b) The stress–strain curves for five different tensile test measurements of the graphite film (t : 13–26 μm) prepared from the stretched PA film $[(\text{CHI}_{0.33-0.36})_n]$ at 2600 $^{\circ}\text{C}$. The load direction is parallel to the stretching direction. The insets show photographs of the carbon film before (upper) and after (lower) the measurement.

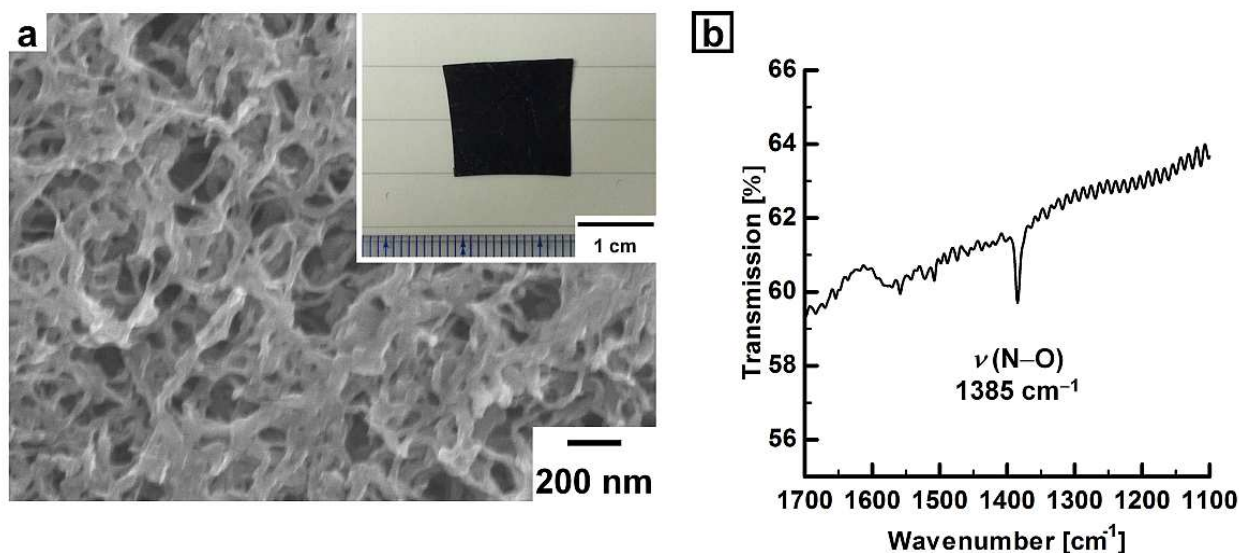


Figure S12. (a) SEM image of the gas side of the graphite nitrate film doped with fuming HNO_3 [$(\text{C}_{268}^+(\text{NO}_3^-))$]. The amount of dopant was determined by weighing the doped graphite films. The graphite film was prepared by carbonization following by heat treatment at 2600°C from the typical PA film [$(\text{CHI}_{0.27})_n$]. The inset shows a photograph of the gas side of the graphite nitrate film (t : $53 \pm 1 \mu\text{m}$, σ : $360 \pm 29 \text{ S/cm}$). The electrical conductivity of the graphite film increased by approximately 35% as a result of the chemical doping. (b) IR absorption spectrum of the graphite nitrate film. The absorption band at 1385 cm^{-1} is attributed to the N–O vibration of the NO_3^- ion.

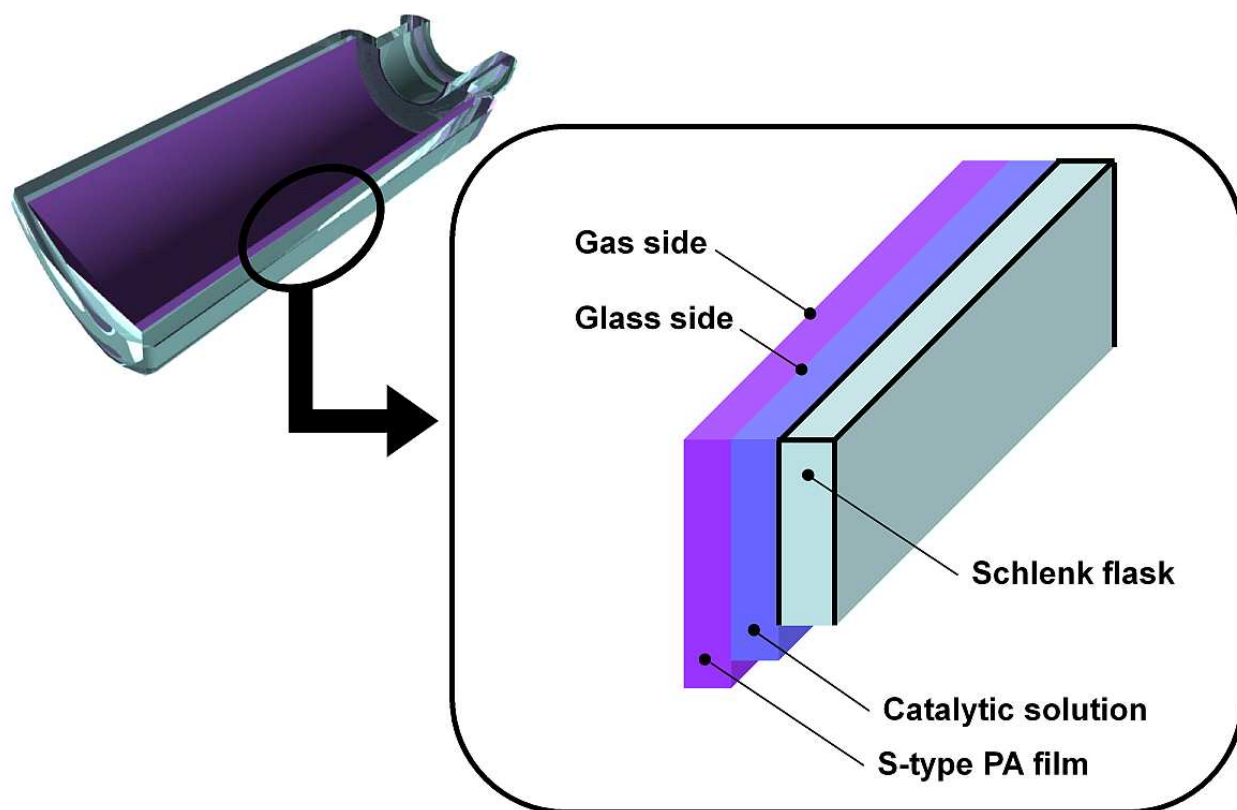


Figure S13. Gas and glass sides of typical PA film.

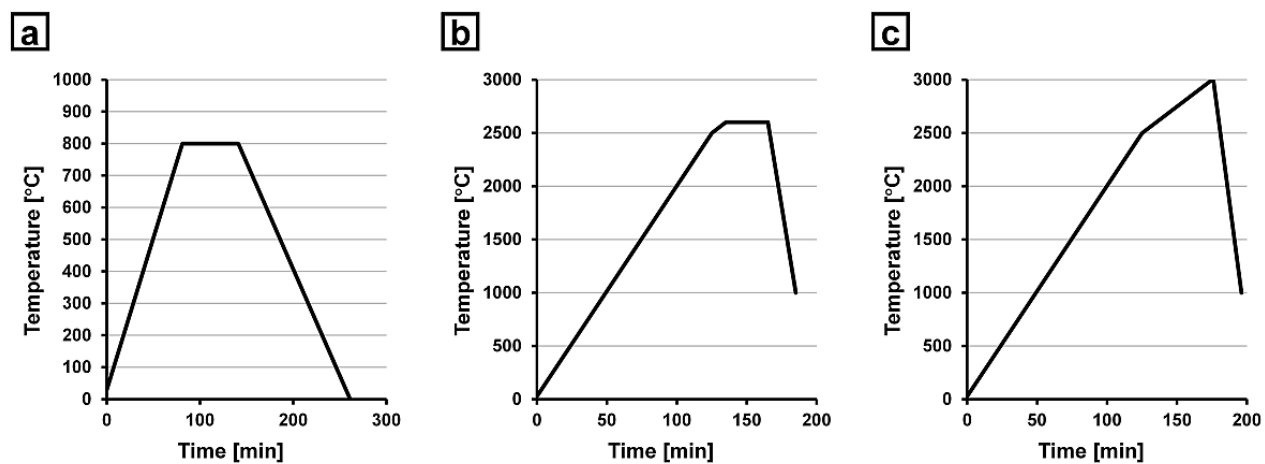


Figure S14. Heat-treatment programs during (a) carbonization at 800 °C and graphitizations at (b) 2600 °C and (c) 3000 °C.

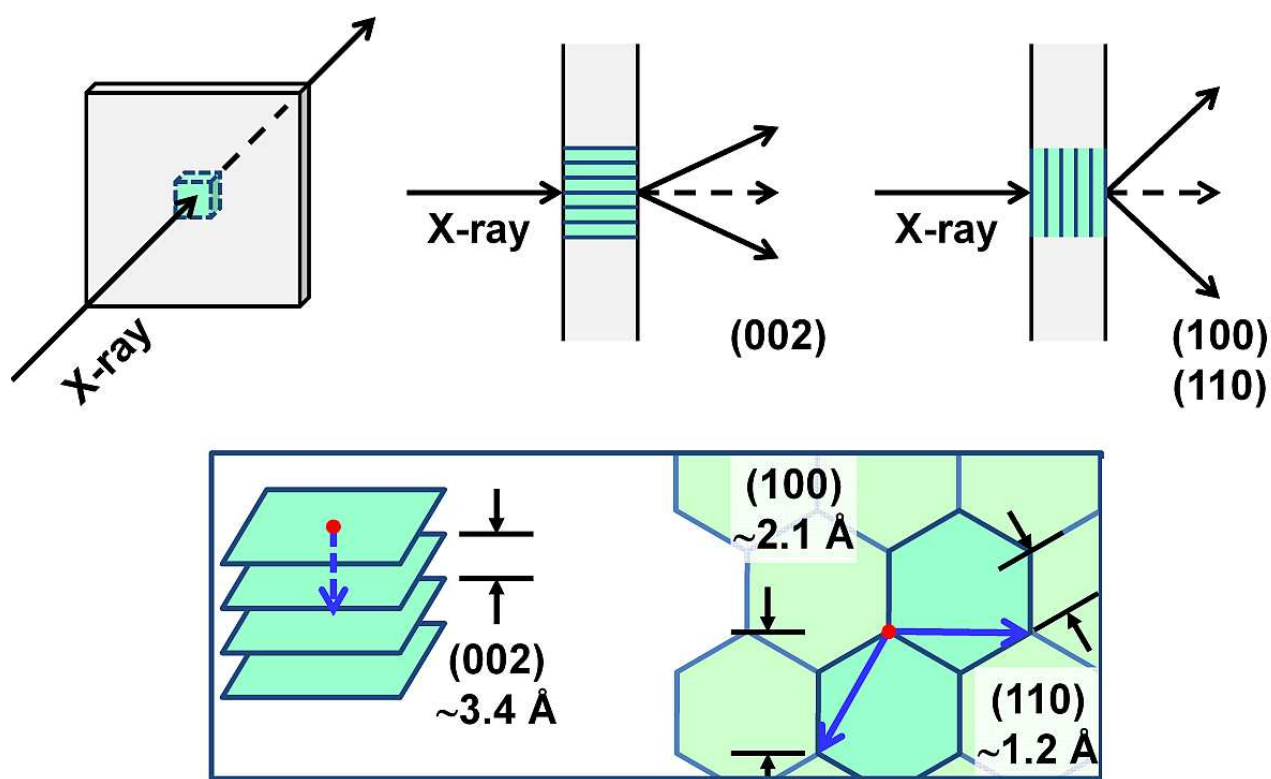


Figure S15. Sample configuration for XRD measurements.

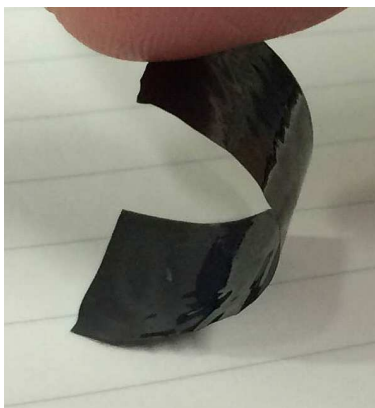


Figure S16. Photograph of the typical PA film ($[\text{CHI}_{0.17}]_n$, t : $60 \pm 11 \text{ } \mu\text{m}$, w : 15 mm, l : 30 mm, σ : $267 \pm 21 \text{ S/cm}$) graphitized at 2600 °C, showing that the film has some bending flexibility.

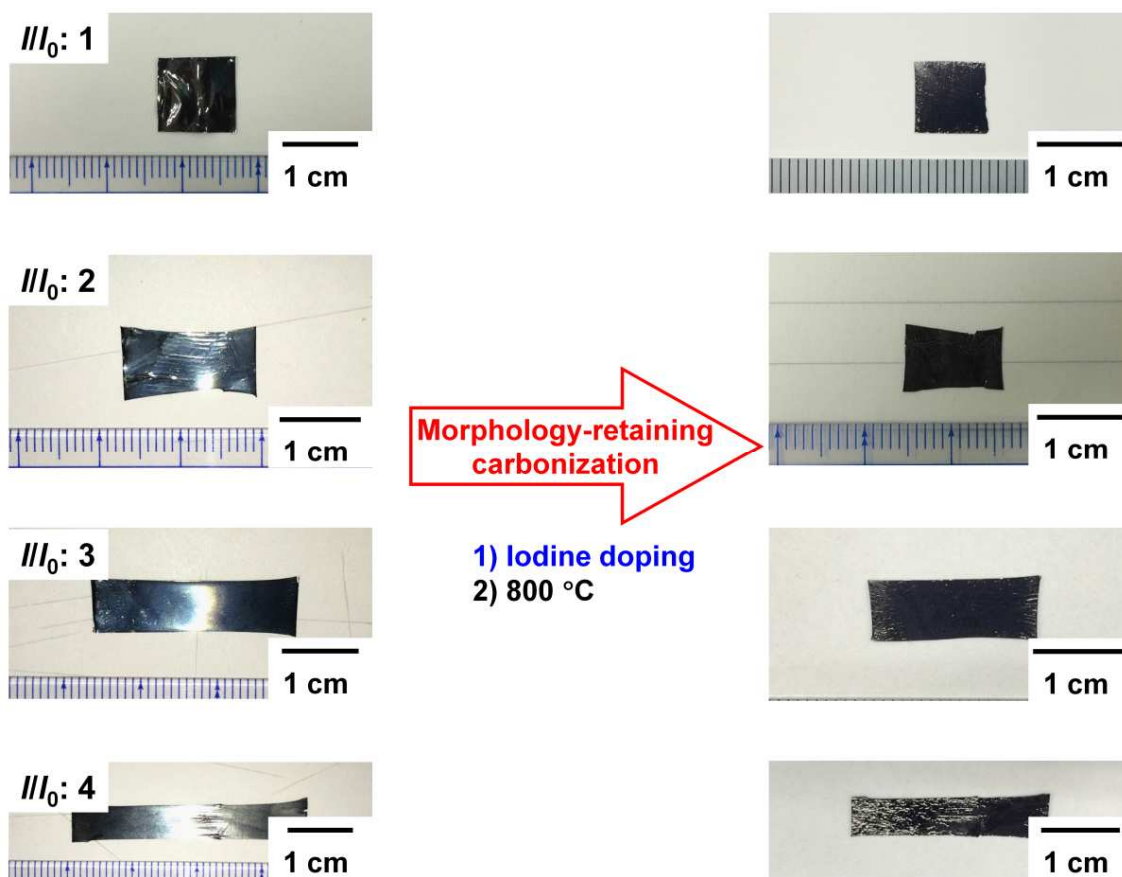


Figure S17. Photographs of the pristine stretchable PA films before the iodine doping with various degree of stretching (l/l_0) before (left) and after (right) the morphology-retaining carbonization at 800 °C.

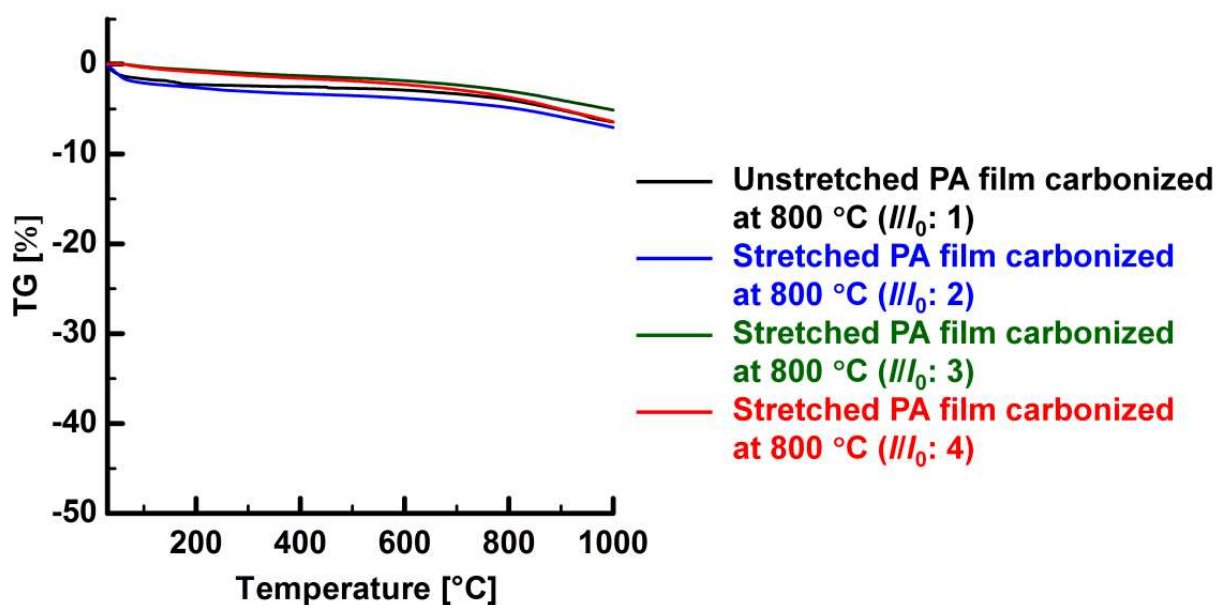


Figure S18. TG curves of the stretchable PA films ($[CHI_{0.39-0.40}]_n$) carbonized at 800 °C (weight loss: 5.1–7.1% up to 1000 °C).

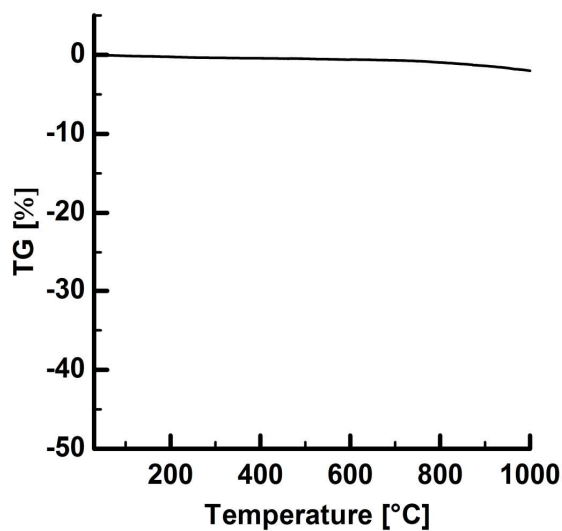


Figure S19. TG curve of the stretched PA film ($[CHI_{0.36}]_n$) graphitized at 2600 °C, indicating the high thermal stability of the film (weight loss: <2.0% up to 1000 °C).

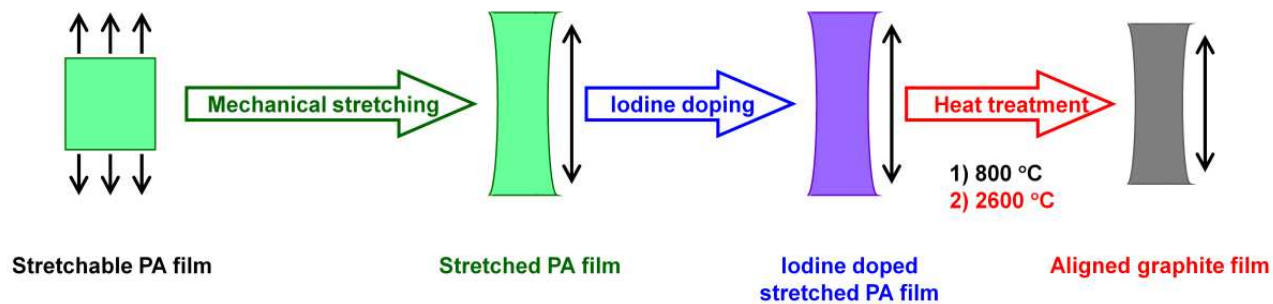


Figure S20. Preparation of a macroscopically aligned graphite film using the carbonization of a stretchable PA film synthesized using a solvent evacuation method.

Table S1. The structural parameters estimated from the XRD patterns of the graphite films prepared at 2600 °C.

Precursor	$[\text{CHI}_x]_n$	Direction or form	d_{002} (Å)	$d_{100\ 101}$ (Å)	$I_{002}/I_{100\ 101}$	L_c (nm)	Number of graphite layers	Orientation factor; f
S-type PA film	0.24–0.27	Through	3.4	2.1	9.0	–	–	–
		Edge	3.4	2.1	15	–	–	–
		In powder	3.4	2.1	11	4.7	14	–
Unstretched PA film	0.26	Through	3.5	2.1	1.3	–	–	–
		Edge	3.4	2.1	155	–	–	<0
		In powder	3.4	2.1	11	5.3	16	–
Stretched PA film	0.33–0.36	Through	3.5	2.1	4.6	–	–	0.28–0.33
		Edge	3.4	2.1	422	–	–	0.77
		In powder	3.4	2.1	25	11	31	–

Table S2. The summary of electrical conductivity of the carbon and graphite films as a function of stretching degree.

Precursor	Heat treatment temp. (°C)	σ (S/cm)		$\sigma_{//}$ (S/cm)	
		$///l_0: 1$	$///l_0: 2$	$///l_0: 3$	$///l_0: 4$
Stretchable PA film	800	23±1 ($t: 76\pm5$ μm)	21±1 (66±10 μm)	25±3 (64±4 μm)	44±3 (26±8 μm)
	2600	282±33 (46±8 μm)	— ^a	—	539±39 (14±0 μm)

^a Data not available.

Table S3. The summary of sheet resistance of the carbon and graphite films.

Precursor	Heat treatment temp. (°C)	Sheet resistance; ρ_s (Ω/\square)	Thickness; t (μm)
S-type PA film	800	5.2±0.3	78±2
	1400	0.93±0.07	73±4
	1800	0.89±0.07	47±4
	2200	0.78±0.06	57±1
	2600	0.69±0.03	60±11
	3000	0.61±0.01	69±3
Unstretched PA film	2600	0.77±0.09	46±8
Stretched PA film		0.68±0.02	26±2